Title : Optimal E-field Vector Combination for a Highly-focused Antenna-array

Authors: Ashwani Sharma, Ignacio J. Garcia Zuazola, MIEEE, Ramon Martinez, MIEEE, John C. Batchelor, SMIEEE, Asier Perallos, MIEEE, and Leandro de-Haro Ariet

The DOI is: 10.1109/LAWP.2014.2306574

Optimal E-field Vector Combination for a Highly-focused Antenna-array

Ashwani Sharma, Ignacio J. Garcia Zuazola, *MIEEE,* Ramón Martinez, *MIEEE,* John C. Batchelor, *SMIEEE,* Asier Perallos, *MIEEE,* and Leandro de-Haro Ariet

Abstract

A near-field highly focused circular phased-array antenna for 5.8 GHz Radio Frequency IDentification (RFID) applications is presented. The Electric field (E-field) at the focus is enhanced by a constructive vector combination in a three dimensional (3-D) coordinate system. The array dipoles of the antenna are oriented to enhance the energy confinement at the focus, and the radii of the circular array is optimized for lower sidelobe levels. As a result, the proposed design achieves an enhanced focalization of $\approx$ 4dB with reduced sidelobe levels of $\approx$ 12dB compared to earlier designs.

Index Terms

Phased-array, planar antenna, near-field, focalization, RFID

I. Introduction

In certain RFID applications, the reader antenna should be highly focused in the Near-Field (NF) region with low Side-Lobe-Levels (SLL) [1]. The focalization leads to high gains with increased efficiency and the low SLLs improve read accuracy and reduce cross talk. The desired NF Focused (NF-F) effect [2]–[8] is achieved by adjusting the phases of the array elements of the antenna so that the radiated fields of every element contribute constructively at the focus. The antenna-array can be implemented using microstrip components with an appropriate feed network [2], [3], [5].

A reader antenna where the focal length is adjustable offers flexibility where the read distance is closely defined and may change. In rectangularly-configured arrays [4], this can be performed by phase shifts between the array elements, but since one phase shifter per element is required, the feeding network becomes complex. In contrast, a circularly-configured array [9] offers a reduced complexity since all the array elements of a circle are equidistant from the focus, and therefore, only one phase shifter per circle is required. In [9] a NF Focused Circular Array (NF-FCA) antenna for 5.8GHz RFID applications consisting of 24 radially oriented array elements (planar printed dipoles) distributed along the periphery of 3 concentric circles (8 elements per circle) was presented. The appropriate phase distribution of the circles confined the radiated energy to the focus. In this paper, the antenna presented in [9], hereby defined as the initial design, is optimized for an enhanced focalization. In Section II-A, the E-fields generated by each dipole of the array are modelled analytically in a 3-D coordinate system. Only 2 cases of dipole orientation are presented for brevity, the radial and the co-linear. The initial design (with radially oriented dipoles) is discussed in Section II-B. It will be shown that though the E-fields from radially oriented dipoles combine constructively at the focus, the focusing effect can be further improved with the design proposed in Section II-C. The enhancement was achieved by reorienting the dipoles of the initial design appropriately for maximum E-field response, while the reduced side lobes were achieved by redefining the internal element radii of the antenna. Results are given in Section III where an improved energy confinement at the focus is observed for the proposed design compared to the initial array.

II. The optimization process using vector projections

The NF-FCA is first modelled using vector projections in a 3-D coordinate system to establish the E-field distribution for given dipole orientations, Fig. 1(a). The antenna-array is located in the X-Y plane and centered at the origin. The focus lies on the Z-axis with coordinates $(0, 0, F)$, where F is the focal length. The array consists of C concentric circular rows (circles) of radii R^v, $\forall\, v \in [1, C]$, where N dipoles are distributed per circle (NC dipoles in total). The antenna-array is analyzed using vector projections onto X, Y, and Z and their respective unit vectors $\hat{x}$, $\hat{y}$, and $\hat{z}$, subsequently.

This work has been partially funded by the European Union through a Predoctoral Research Grant (FPI-Deusto 2011-2015). Ashwani Sharma, Ramón Martinez, and Leandro de-Haro (SSR Department, Universidad Politécnica de Madrid ETSIT, Ciudad Universitaria, 28040, Madrid, Spain); Ashwani Sharma, Ignacio J. Garcia Zuazola, and Asier Perallos (Deusto Institute of Technology - DeustoTech, University of Deusto, 48007, Bilbao, Spain); John C. Batchelor (Department of Engineering and Digital arts, University of Kent, Canterbury, Kent, CT2 7NT, UK). Email: {ashwani.sharma,i.j.garcia,perallos}@deusto.es,{ramon, leandro}@gr.ssr.upm.es, j.c.batchelor@kent.ac.uk.

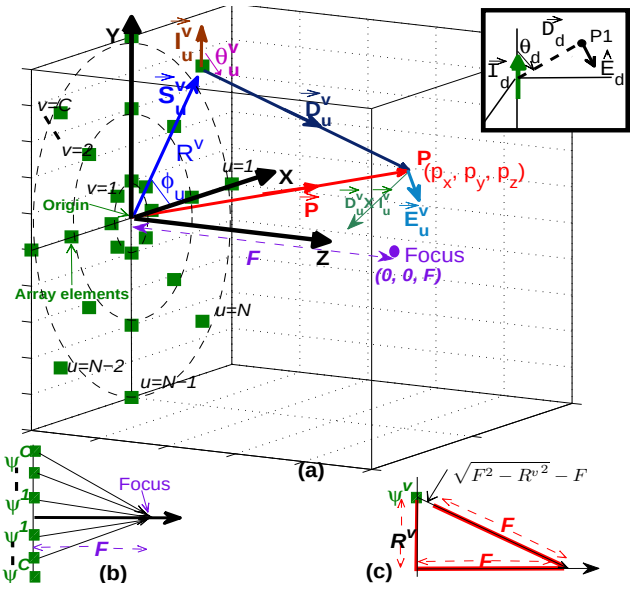

Fig. 1. (a) The NF-FCA antenna E-field vector projections in a 3-D rectangular coordinate system. (b) A 2-D representation of the array elements (phases ,ψ) in regard to the focus and (c) Geometric evaluation of the ψ^v corresponding to a circle v.

A. The 3-D vector projection - analytical model

In this section, the contribution due to each dipole of the NF-FCA shown in Fig. 1 is formulated. Let $\vec{S}_u^v$ be the spacial location of a dipole u in a circle v, and given by:

$$\vec{S}_u^v = (R^v \cos\phi_u)\,\hat{x} + (R^v \sin\phi_u)\,\hat{y} + 0\hat{z}, \tag{1}$$

where $u \in [1, N]$; $v \in [1, C]$, and ϕ_u is the angular position of dipole u with respect to the X-axis. The direction of the E-fields at the focus is governed by the orientation of every dipole element and represented by the current vector $\vec{I}_u^v$ with direction, $\hat{I}_u^v$, and magnitude, I_u^v. Since the E-fields originating from each dipole are aimed to sum constructively at the focus, the current phases, ψ^v are adjusted to compensate for the unequally distant dipoles, Fig. 1(b). While the dipoles in a shared circle are equally distant from the focus and share the same phase (ψ^v), a phase difference is necessary between dipoles of different circles, hence, $C-1$ phase shifters are required. ψ^v is determined from the geometry of Fig. 1(c) and expressed as:

$$\psi^v = -k_0\left(\sqrt{F^2 + R^{v\,2}} - F\right), \tag{2}$$

where $k_0 = \frac{2\pi}{\lambda}$ is the wave number in free space and λ the wavelength. Using a known total array current, I_0, with the phase shifts, ψ^v, the I_u^v can be calculated from (2) as

$$I_u^v = \frac{I_0}{NC}\left(e^{-jk_0\psi^v}\right), \quad \forall\, u \in [1, N]\,;\, v \in [1, C]\,. \tag{3}$$

We note from (3) that, I_u^v is independent of u for a given v because ψ^v is constant for all the dipoles in a circle v. $\hat{I}_u^v$ is found given the orientation of the dipoles in the array. Therefore, the NF-FCA antenna can be fully described using N, C, R^v, ϕ_u, $\vec{S}_u^v$, and $\vec{I}_u^v$. The resulting E-field at a point P due to NC dipoles, Fig. 1(a), is subsequently formulated. The vector location of P is denoted as $\vec{P} = p_x\hat{x} + p_y\hat{y} + p_z\hat{z}$ and the vector distance, $\vec{D}_u^v$, between the dipole u (of the circle v) and the point P, is given by:

$$\vec{D}_u^v = \vec{P} - \vec{S}_u^v. \tag{4}$$

As we consider distances of F between 0.4 to 2 m, according to [9], the focus is in the far-field of each dipole element. Therefore the E-field vector of every dipole in isolation can be expressed using a local spherical coordinate system [10]:

$$\vec{E}_d = \frac{j\eta I_d e^{-jk_0 D_d}}{2\pi D_d}\left(\frac{\cos\left(\frac{\pi}{2}\cos\theta_d\right)}{\sin\theta_d}\right)\hat{E}_d, \tag{5}$$

where $\eta = 120\pi$, θ_d is the angle between the dipole current vector, $\vec{I}_d$ with respect to $\vec{D}_d$ (distance vector to P1), and the quantities in the dipole local coordinate system are denoted with the subscript d. The direction of $\vec{E}_d$ is shown in Fig. 1(a) (inset), and since we consider a rectangular coordinate system, (5) is mapped to $\vec{E}_u^v$ (the field vector at point P due to dipole u of the circle v) as follows:

$$\vec{E}_u^v = E_u^v \hat{E}_u^v, \tag{6}$$

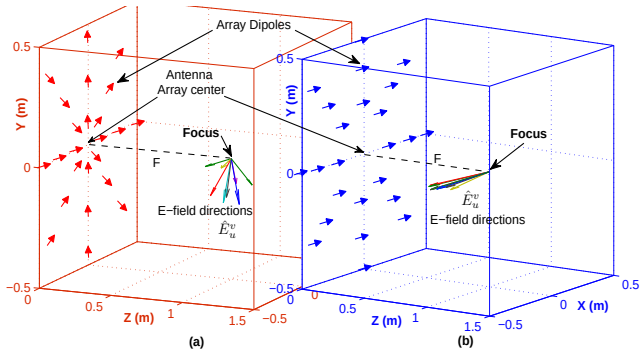

Fig. 2. E-field vectors at the array focus due to (a) radially oriented dipoles (initial design), (b) co-linearly oriented dipoles (proposed design).

where E_u^v, and $\hat{E}_u^v$ are the magnitude, and the direction respectively. E_u^v is calculated using (5), where D_d is substituted by the magnitude D_u^v from (4), and θ_d is substituted by θ_u^v, which is computed by the cosine law as:

$$\theta_u^v = \cos^{-1}\left(\frac{\vec{D}_u^v \cdot \vec{I}_u^v}{D_u^v I_u^v}\right). \tag{7}$$

Using (4) and (7) we derive E_u^v from (5) as:

$$E_u^v = \frac{j\eta I_u^v e^{-jk_0 D_u^v}}{2\pi D_u^v} \frac{\cos\left(\frac{\pi}{2}\cos\theta_u^v\right)}{\sin\theta_u^v}\left(e^{-jk_0\psi^v}\right), \tag{8}$$

where $e^{-jk_0\psi^v}$ is the phase shift required to co-phase E-fields at the focus. According to the inset of Fig. 1(a), $\hat{E}_u^v$ must be normal to $\vec{D}_u^v$ and parallel to the plane determined by $\vec{D}_u^v$ and $\vec{I}_u^v$. This condition is satisfied using vector cross products:

$$\hat{E}_u^v = \frac{\vec{D}_u^v \times \left(\vec{D}_u^v \times \vec{I}_u^v\right)}{|\vec{D}_u^v \times \left(\vec{D}_u^v \times \vec{I}_u^v\right)|} = \frac{\vec{D}_u^v\left(\vec{D}_u^v \cdot \vec{I}_u^v\right) - \vec{I}_u^v D_u^{v2}}{|\vec{D}_u^v\left(\vec{D}_u^v \cdot \vec{I}_u^v\right) - \vec{I}_u^v D_u^{v2}|}. \tag{9}$$

Finally, summing the E-field vectors, $\vec{E}_u^v \;\forall u \in [1, N]\,; v \in [1, C]$ (6), found from (8) and (9), the overall E-field, $\vec{E}$, at P is calculated as:

$$\vec{E} = \sum_{v=1}^{C}\sum_{u=1}^{N} \vec{E}_u^v = \sum_{v=1}^{C}\sum_{u=1}^{N} E_u^v \hat{E}_u^v. \tag{10}$$

B. Initial NF-FCA antenna design

The initial design consists of 3 circles ($C = 3$), each with 8 uniformly separated dipoles ($N = 8$) and circle radii $R^1 = 10$ cm, $R^2 = 30$ cm, and $R^3 = 50$ cm. Hence, the array consists of $NC = 24$ printed dipoles assembled on the X-Y plane, Fig. 1(a). The angular positions ϕ_u of vectors $\vec{S}_u^v$ are calculated using (1), where $\phi_u = \frac{2\pi(u-1)}{N}$. As in [9], we considered radially oriented dipoles, Fig. 2(a). Hence, $\hat{I}_u^v = s\hat{S}_u^v$, where $s = -1$ for $u > 5$ and $s = 1$ otherwise. The phases of the array elements were calculated using (2) and the feeding network of [9] incorporated. The total E-field of the initial design was calculated using (10).

C. Proposed NF-FCA antenna design

The proposed design is now presented. Based on the initial design and using the customized 3-D vector projection analytical model of Section II-A, various dipole orientations were investigated. The optimization process was conducted, first, by finding the optimal dipole orientation for the maximum summation of the E-Field at the focus, and next, by improving the side lobes in the focal plane without compromising the focalization performance. This was realized by an intermediate design ID-1 and the proposed design respectively. It was found that least cancellation of $\hat{E}_u^v$ occurred when all dipoles were aligned in parallel (co-linearly oriented), Fig. 2(b). Although the co-linear dipole orientation led to an enhanced power at the focus, the resulting antenna Forward-Lobe-Levels (FLLs) and SLLs were compromised in the intermediate design ID-1. To compensate for the poor FLLs and SLLs achieved by ID-1 (results are given in Section III), R^1 and R^2 were optimized using the model of Section II-A with iteration $0 < R^2 < R^3$ and $0 < R^1 < R^2$ respectively, which offered the most appropriate FLLs and SLLs without compromising the focalization of ID-1 and conducted to the proposed design. These gave the optimal radii that are shown in Fig.2 (b).

The shared design parameters of the initial and the proposed designs are: 24 dipoles, $N = 8$, $C = 3$, and ϕ_u; while the new set of optimized R^v is: $R^1 = 22$cm, $R^2 = 37$cm, and $R^3 = 50$cm (maximum antenna size). ID-2 is presented in Section III to show how the initial design performs when the former R^1 and R^2 values are used. As the dipoles are co-linear, $\hat{I}_u^v = \hat{S}_1^v$, and $\vec{S}_u^v$ is given by (1). Therefore, the total E-field distributions for the given designs are calculated using (10), and compared to that of the initial design. For a fair comparison between the designs, the same input power, same number of dipoles (24 elements) and same antenna dimension R^3 were used. The results are presented in Section III.

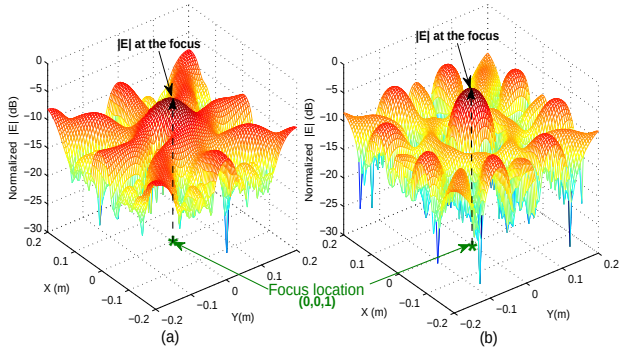

Fig. 3. Normalized field strength $|E|$ distribution (analytical) in the focal plane when $F = z = 1$ m (a) initial design (b) proposed design.

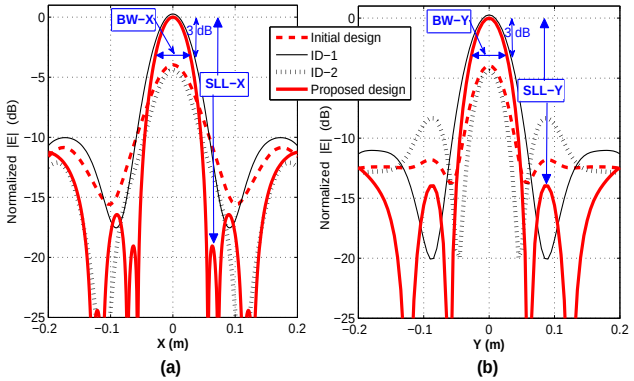

Fig. 4. The normalized $|E|$ (analytical) for two transversal cuts of the main beam, $z = F = 1$ m along the (a)X-axis (b)Y-axis.

III. Analytical Results

Results for the ID-1, -2 and the final designs outlined above are now presented. We use the 3-D vector projection model presented in Section II-A aided by MATLAB for the analysis. The expected E-field distribution in the near-field region of Fig. 1(a) is computed using (10) and the required ψ^v using (2). For $F = 1$m, the calculated ψ^v at each circle R^1, R^2, and R^3 of the array are respectively, 0.92π, 2.56π, 4.56π, for the initial and ID-1 designs, and 0.19π, 1.70π, 4.56π, for the final and ID-2 designs. The normalized field strength $|E|$ distribution in the focal plane when $z = F = 1$m for the initial and the proposed design is presented in Fig 3(a) and (b), respectively.

The $|E|$, the beam-width (BW), focal depth, SLL and FLL of the designs are evaluated with the following expressions:

$$\text{BW} = \Delta\left[arg_{(x,y)}(|E|_{dB}^{(x,y,F)} = |E|_{dB}^{(0,0,F)} - 3)\right],$$

$$\text{focal depth} = \Delta\left[arg_{(z)}(|E|_{dB}^{(0,0,z)} = |E|_{dB}^{(0,0,F)} - 3)\right],$$

$$\text{SLL} = |E|_{dB}^{(x_0,y_0,F)} - |E|_{dB}^{(0,0,F)},$$

$$\text{FLL} = |E|_{dB}^{(0,0,z_0)} - |E|_{dB}^{(0,0,F)},$$

where $\Delta[p]$ is the distance between two possible solution points p, and (x_0, y_0, z_0) are the coordinates of the lobe close to the focus under consideration.

The normalized $|E|$ of the initial, ID-1, ID-2, and proposed design showing two transversal cuts of the main beam in Cartesian form is depicted in Fig 4. Compared to the initial design, the ID-1 presents higher $|E|$ levels at the expense of higher SLLs, and the proposed design compensates this as a result of the optimized R^1 and R^2. ID-2 is shown to corroborate fair comparison to the initial design with the optimized radii from Section II-C. There are similar $|E|$ levels for the initial and the ID-2 designs, though compared to the initial, the proposed design shows a 4.02dB higher $|E|$ (measured at boresight, i.e. the focus). There are lower first-SLLs along the X-axis (SLL-X) and the Y-axis (SLL-Y), with narrower BWs in the X-axis (BW-X) and similar in the Y-axis (BW-Y).

The tunable focusing ability of the initial and the proposed design in the Z-axis $(x = 0, y = 0)$ is compared for various F (0.6, 0.8, and 1m) and presented in Fig. 5. For the representation, the patterns are normalized to the $|E|$ of the proposed design when $F = 1$m. The figure shows (in the three F cases) about a 4dB higher $|E|$ with lower FLLs in the proposed design; this defines the highly-focused antenna-array.

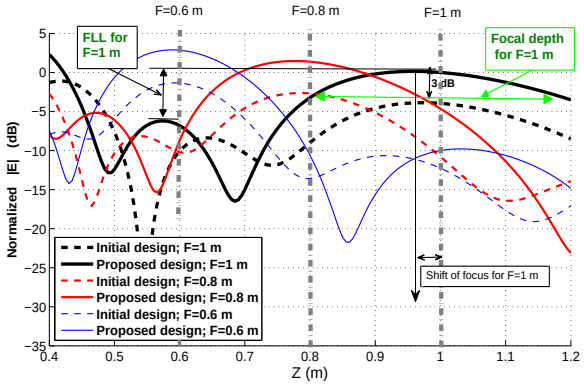

Fig. 5. The tunable focusing ability comparison (analytical) of the initial and the proposed design in the Z-axis ($x = 0, y = 0$) for various F.

A detailed comparison between the designs is presented in Table I which includes the side interference performance of the two, quantified by the maximum SLL (SLL-Max) at the focal plane, Fig 3. The results give confidence of an improved focalization for the proposed design, which compared to the initial design has: (1) $\approx$ 4dB higher $|E|$ in all the evaluated Fs, (2) narrower BW-X and similar BW-Y, (3) lower SLL-X, SLL-Y and SLL-Max, with similar FLL when $F < 0.6$m, and lower FLL when $F > 0.6$m, (4) higher focal depths of $\approx$ 4cm. The focal depth is defined between the -3dB points of the main lobe close to the focus and along the z-axis, Fig 5. The difference in focal depth between the designs was 10-15% higher for the proposed design and is deemed acceptable for the antenna-array application. Owing to the small span of F (0.6 to 1m), the pathloss (in the 5.8GHz near-field) is relatively low (in the order of $\approx$ 0.05dB/0.1m) which is the reason the 4dB enhancement is present in the three F cases. The main lobes shown in Fig 5 were slightly shifted from the focus and was due to a field spreading factor [11]. This is in line with the results reported in [5], [9], [12]. The calculated shifts of the focus, measured in percentage (%), are given by $\frac{\text{shift}(m)}{F(m)} \times 100$ and provided in Table I. The calculated values provide an insight for correction prior to manufacture.

TABLE I
COMPARISON BETWEEN THE INITIAL DESIGN AND THE PROPOSED DESIGN

focal length, $F \rightarrow$	0.5 m	0.6 m	0.8 m	1 m
Initial design:-				
BW-X (cm)	5.10	5.50	6.50	7.70
BW-Y (cm)	3.30	3.70	4.50	5.50
SLL-X (dB)	−7.35	−7.19	−7.01	−6.89
SLL-Y (dB)	−7.90	−7.89	−7.86	−7.82
SLL-Max (dB)	−2.27	−2.29	−3.08	−3.14
FLL (dB)	−5.85	−6.27	−5.54	−4.50
Focal depth (cm)	13.30	16.10	23.50	31.70
% shift of the focus	0.4	0.6	2.0	3.6
Proposed design:-				
BW-X (cm)	3.32	4.24	4.56	5.42
BW-Y (cm)	3.12	3.55	4.42	5.32
SLL-X (dB)	−14.28	−15.37	−17.36	−19.04
SLL-Y (dB)	−9.83	−11.06	−12.81	−13.91
SLL-Max (dB)	−3.91	−3.89	−3.81	−3.80
FLL (dB)	−5.45	−6.17	−6.23	−6.35
Focal depth (cm)	15.20	20.15	26.75	36.75
% shift of the focus	1.6	2.0	2.8	4.2
E-field enhancement (dB) $\lvert E\rvert$proposed - $\lvert E\rvert$initial	4.29	4.22	4.10	4.02

IV. CONCLUSION

The appropriate modelling of E-field vectors projected by an antenna-array were analyzed in a 3-D coordinate system for optimal field strength near to its focus. Using the developed 3-D vector projection model, an initial 5.8 GHz NF-FCA antenna of planar-printed dipoles was validated and subsequently optimized by a constructive arrangement of the element orientations. The model affirms that arrays with co-linearly oriented dipoles outperform similar designs with radially oriented dipoles, and the corresponding design parameters for the optimization were provided. Tags over conveyor belts are likely to be consistently identically oriented (i.e. always vertical or horizontal on food packaging) and the single linear polarization that is excited by the proposed antenna-array would be suitable for such an RFID application. Although reorientating the dipoles improved the

focusing of the antenna-array for a range of F, the FLL and SLL were compromised and improved patterns were obtained by adjusting the radii of R^1 and R^2. The resulting shift in the focus (also present in the initial design) can be compensated by fine-tuning of the phase shifters in the antenna-array.

REFERENCES

[1] K. Chen, S. Zhong, X. Tang, and Z. Sun, "Low-sidelobe circularly-polarized microstrip array for RFID reader applications," in *Proc. IET Conf. Wireless, Mobile and Sensor Networks*, Shanghai, China, Dec. 2007, pp. 482–484.

[2] M. Bogosanovic and A. G. Williamson, "Microstrip antenna array with a beam focused in the near-field zone for application in noncontact microwave industrial inspection," *IEEE Trans. on Instrumentation and Measurement*, vol. 56, no. 6, pp. 2186–2195, Dec. 2007.

[3] M. Bogosanovic and A. G. Williamson, "Antenna array with beam focused in near-field zone," *Electron. Lett.*, vol. 39, no. 9, pp. 704–705, May 2003.

[4] A. Buffi, A. A. Serra, P. Nepa, H.-T. Chou, and G. Manara, "A focused planar microstrip array for 2.4 GHz RFID readers," *IEEE Trans. Antennas Propag.*, vol. 58, no. 5, pp. 1536–1544, Mat 2010.

[5] S. Karimkashi and A. A. Kishk, "Focused microstrip array antenna using a DolphChebyshev near-field design," *IEEE Trans. Antennas Propag.*, vol. 57, no. 12, pp. 3813–3820, Dec. 2009.

[6] A. Buffi, A. Serra, P. Nepa, G. Manara, and M. Luise, "Near field focused microstrip arrays for gate access control systems," in *Proc. IEEE APSURSI*, Charleston, SC, USA, June 2009, pp. 1–4.

[7] S. M. Roy N. C. Karmakar and M. S. Ikram, "Development of smart antenna for rfid reader," in *Proc. IEEE Int. Conf. RFID*, Las Vegas, Nevada, USA, May 2008, pp. 65–73.

[8] S. H. Zainud-Deen, H. A. Malhat, and K. H. Awadalla, "Dielectric resonator antenna phased array for fixed RFID reader in near field region," in *Proc. Japan-Egypt Conference on Electronics, Communications and Computers*, Alexandria, Egypt, Mar. 2012, pp. 102–107.

[9] R. Siragusa, P. Lematre-Auger, and S. Tedjini, "Tunable near-field focused circular phase-array antenna for 5.8-ghz rfid applications," *IEEE Antennas and Wireless Propagation Letters*, vol. 10, pp. 33–36, 2011.

[10] C. A. Balanis, *Antenna Theory Analysis and Design*, Wiley, 2 edition, 1997.

[11] A. Buffi, P. Nepa, and G. Manara, "Design criteria for near-field-focused planar arrays," *IEEE Antennas and Propagation Magazine*, vol. 54, no. 1, pp. 40–50, Feb. 2012.

[12] J. W. Sherman, "Properties of focused aperture in the fresnel region," *IRE Trans. Antennas Propag*, vol. 10, no. 4, pp. 399–408, Jul. 1962.